Scattering of Plane Waves by an Anisotropic Dielectric Half-Plane

Arslan Yazici, *Member, IEEE,* and A. Hamit Serbest, *Senior Member, IEEE*

***Abstract*— Scattering of plane waves by a semi-infinite anisotropic thin dielectric layer is investigated, which can be considered as an example for electromagnetic energy absorbing materials. A pair of second-order boundary conditions is used to simulate an anisotropic thin dielectric layer as an infinitesimally thin sheet. Formulation is based on the Fourier integral transform technique, which reduces the scattering problem to two decoupled scalar Wiener–Hopf equations. Diffracted, reflected, and transmitted field terms are evaluated by using the Wiener–Hopf solutions that is obtained by the standard method. The uniqueness of the solution is satisfied by imposing an edge constraint in addition to the classical edge condition.**

***Index Terms*—Electromagnetic scattering by anisotropic media.**

I. Introduction

As is well known, due to absorbing characteristics of dielectrics, scattering by such structures has great importance in electromagnetic theory and also scattering by a dielectric half-plane or strip yields canonical solutions for the geometrical theory of diffraction (GTD) analysis of dielectric covered complex structures. Diffraction problems have been considered by various authors via simulating the dielectric slab by different types of approximate boundary conditions. Early studies are due to Senior [1] and Anderson [2] where half-plane diffraction problem was considered by using standard resistive sheet boundary conditions, which holds only electric current on the sheet and provides an effective simulation under many circumstances. Regarding the decrease in accuracy at oblique angles of incidence when the electric vector has a component perpendicular to the layer, Senior and Volakis [3] had introduced a modified conductive sheet in addition to the resistive one to improve the simulation. On the other hand, a pair of boundary conditions was introduced by İdemen [4] to simulate a special type of anisotropic dielectric layer that is homogenous and isotropic with respect to the directions parallel and perpendicular to the plane, while the half-spaces lying beneath and above the layer are homogenous and isotropic media as shown in Fig. 1. The boundary conditions on an infinitesimally thin anisotropic dielectric sheet placed in free-space are as follows:

$$\vec{n}\times(\vec{H}^{+}-\vec{H}^{-})=A(\vec{E}_t^{+}+\vec{E}_t^{-})+B\vec{n}\times\text{grad}(H_n^{+}+H_n^{-}) \tag{1}$$

Manuscript received March 19, 1996; revised December 2, 1996.

The authors are with the Department of Electrical and Electronics Engineering, Cukurova University, Balcali, Adana, 01330 Turkey.

Publisher Item Identifier S 0018-926X(99)07077-5.

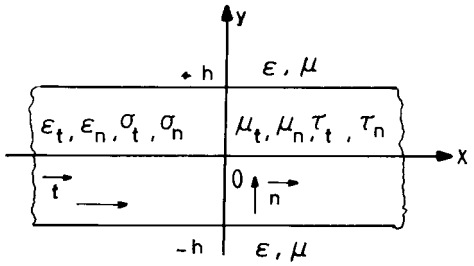

Fig. 1. Anisotropic dielectric layer thickness $2h$.

and

$$\vec{n}\times(\vec{E}^{+}-\vec{E}^{-})=C(\vec{H}_t^{+}+\vec{H}_t^{-})+D\vec{n}\times\text{grad}(E_n^{+}+E_n^{-}) \tag{2}$$

for a layer of thickness $2h$ with $\vec{n}$ denoting the unit vector normal to the layer; and, also it is assumed that $2h<\lambda$ where λ is the wavelength. The constant coefficients in (1) and (2) are

$$\begin{aligned} A&=-i\omega h(\epsilon_t'-\epsilon_0), & B&=-h(\mu_n'-\mu_0)/\mu_n' \\ C&=i\omega h(\mu_t'-\mu_0), & D&=-h(\epsilon_n'-\epsilon_0)/\epsilon_n' \end{aligned} \tag{3}$$

where the index t and n denote the tangential and normal components of the field and the constitutive parameters while $(+)$ and $(-)$ signs denote the limit values of the field when approaching to the sheet from upper and lower sides, respectively. The constitutive parameters are defined as

$$\begin{aligned} \epsilon_t'&=\epsilon_t+i\sigma_t/\omega, & \epsilon_n'&=\epsilon_n+i\sigma_n/\omega \\ \mu_t'&=\mu_t+i\tau_t/\omega, & \mu_n'&=\mu_n+i\tau_n/\omega \end{aligned}$$

where ϵ_t, μ_t, σ_t, τ_t are the dielectric permittivity, magnetic permeability, and electric and magnetic conductivities of the layer in the direction parallel to the plane and ϵ_n, μ_n, σ_n, τ_n are the parameters in the direction normal to the plane.

In this paper, the scattering of electromagnetic waves by an anisotropic dielectric half-plane is investigated, where the simulation is done by the second-order boundary conditions given in (1) and (2). These conditions have the same mathematical form with higher order boundary conditions, which involve second-order derivatives and they can be considered as finite-order approximations of generalized transition conditions (GTC) [5]. The physical interpretation of the factors appearing in the expressions of the two type of conditions are different and anisotropic dielectric layer conditions provide an additional facility to consider the constitutive parameters in the directions parallel and perpendicular to the layer as being

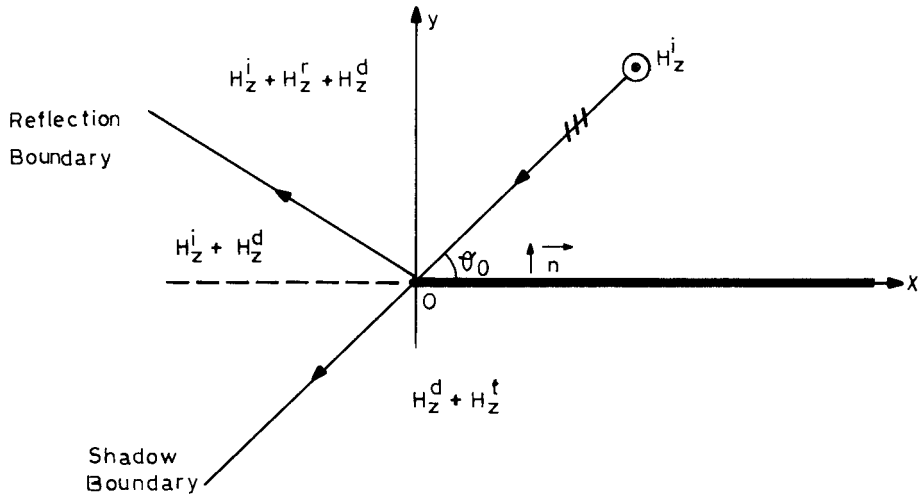

Fig. 2. Geometry of the equivalent boundary-value problem and incident field.

unequal to each other [6]. The formulation of the boundary-value problem is based on the Fourier transform technique and is reduced to two decoupled scalar Wiener–Hopf equations and the solution is obtained by the classical Wiener–Hopf procedure. Since the order of the highest derivative appearing in the boundary conditions is two, the solution involves two unknown constants as expected. One of them is determined by the application of the standard edge conditions, and the second unknown is obtained by imposing the additional transition condition introduced by Senior (see [5]). Finally, the field analysis is derived and numerical results for the solution are presented.

II. The Boundary-Value Problem

The boundary-value problem involves an infinitesimally thin half-plane with the anisotropic dielectric layer conditions being imposed and an H-polarized plane wave incident in the plane perpendicular to the edge (see Fig. 2)

$$H_z^i(x, y) = \exp\{-ik(x\cos\theta_0 + y\sin\theta_0)\} \tag{4}$$

where $0 \leq \theta_0 \leq \pi$. The time dependence is assumed as $\exp(-i\omega t)$ and suppressed throughout the analysis. As known, according to Maxwell's equations, the other nonzero components of the incident field are $E_x^i(x, y)$ and $E_y^i(x, y)$. For the sake of analytical convenience, it is assumed that the surrounding medium is slightly lossy and consequently the wave number has a small positive imaginary part. After completing the analysis, the results corresponding to the lossless case can easily be obtained by writing $\mathrm{Im}(k) \to 0$ in the solution.

The boundary conditions given by (1) and (2) are written as follows for the H-polarized case:

$$[H_z^+ - H_z^-] + \frac{1}{ik\gamma}\frac{\partial}{\partial y}[H_z^+ + H_z^-] = 0, \qquad x > 0 \tag{5}$$

and

$$\frac{\partial}{\partial y}[H_z^+ - H_z^-] + \frac{1}{ik(\gamma_1 + \gamma_2)} \cdot \left[\frac{\partial^2}{\partial y^2} - k^2(\gamma_1\gamma_2)\right][H_z^+ + H_z^-] = 0, \qquad x > 0 \tag{6}$$

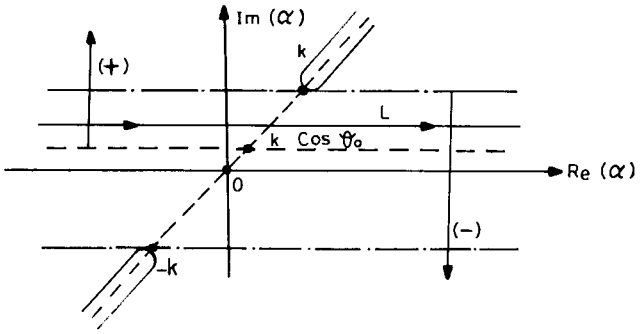

Fig. 3. Regularity band $\mathrm{Im}(k\cos\theta_0) < \mathrm{Im}(\alpha) < \mathrm{Im}(k)$ in complex α-plane and integration line L.

where (5) and (6) are in forms of first- and second-order GTC, respectively, and the parameters are given by

$$\gamma_1\gamma_2 = -(1 + iC/kDZ_0)$$
$$\gamma_1 + \gamma_2 = -1/ikD$$

and

$$\gamma = 1/AZ_0. \tag{7}$$

Since the boundary conditions do not involve the coefficient B in (3), it is expected that magnetic permeability and conductivity in the direction normal to the layer will not be effective in H polarization. The total field is written as the sum of the incident and scattered fields for all y

$$H_z(x, y) = H_z^i(x, y) + H_z^s(x, y) \tag{8}$$

and the following integral representation is introduced for the scattered field:

$$H_z^s(x, y) = \begin{cases} \displaystyle\int_L M(\alpha)e^{i\Gamma(\alpha)y - i\alpha x}\, d\alpha, & y > 0 \\ \displaystyle\int_L N(\alpha)e^{-i\Gamma(\alpha)y - i\alpha x}\, d\alpha, & y < 0 \end{cases} \tag{9}$$

which satisfies the radiation condition for $|y| \to \infty$. Here, $M(\alpha)$ and $N(\alpha)$ are the spectral amplitudes to be determined, and the integration line L given in (9) is any line which is parallel to the $\mathrm{Re}(\alpha)$ axis in the regularity band $\mathrm{Im}(k\cos\theta_0) < \mathrm{Im}(\alpha) < \mathrm{Im}(k)$. The square-root function $\Gamma(\alpha) = \sqrt{k^2 - \alpha^2}$ is defined in the cut complex α-plane such that $\Gamma(0) = k$ (see Fig. 3).

By inserting (4) and (9) into the boundary conditions for $x > 0$ and continuity conditions for $x < 0$ and inverting the resulting integral equations, the following set of equations are obtained:

$$\frac{\Gamma(\alpha)}{k}\left[\frac{k}{\Gamma(\alpha)}+\frac{1}{\gamma}\right][M(\alpha)-N(\alpha)] = \Phi_1^-(\alpha) - \frac{\sin\theta_0}{i\pi\gamma(\alpha - k\cos\theta_0)} \tag{10}$$

$$\left[\Gamma(\alpha)+\frac{\Gamma^2(\alpha)}{k(\gamma_1+\gamma_2)}+\frac{k(\gamma_1\gamma_2)}{(\gamma_1+\gamma_2)}\right][M(\alpha)+N(\alpha)] = \Phi_2^-(\alpha) + \frac{k(\gamma_1\gamma_2+\sin^2\theta_0)}{i\pi(\gamma_1+\gamma_2)(\alpha - k\cos\theta_0)} \tag{11}$$

$$M(\alpha) - N(\alpha) = \Phi_1^+(\alpha) \tag{12}$$

$$\Gamma(\alpha)[M(\alpha)+N(\alpha)] = \Phi_2^+(\alpha). \tag{13}$$

The functions $\Phi_1^{\pm}(\alpha)$ and $\Phi_2^{\pm}(\alpha)$ are unknown functions where $\Phi_{1,2}^+(\alpha)$ are regular in the upper complex α-plane for $\mathrm{Im}(\alpha) > \mathrm{Im}(k\cos\theta_0)$ and $\Phi_{1,2}^-(\alpha)$ are regular in the lower complex α-plane for $\mathrm{Im}(\alpha) < \mathrm{Im}(k)$. Elimination of $M(\alpha)$ and $N(\alpha)$ yields a 2×2 matrix Wiener–Hopf system which can easily be written explicitly as two scalar Wiener–Hopf equations

$$\frac{\Gamma(\alpha)}{k}\cdot\frac{\Phi_1^+(\alpha)}{K_1(\alpha)} - \Phi_1^-(\alpha) = -\frac{\sin\theta_0}{i\pi\gamma(\alpha - k\cos\theta_0)} \tag{14}$$

and

$$\frac{(\gamma_1\gamma_2)}{(\gamma_1+\gamma_2)}\cdot\frac{\Gamma(\alpha)}{k}\cdot\frac{\Phi_2^+(\alpha)}{K_2(\alpha)} - \Phi_2^-(\alpha) = \frac{k(\gamma_1\gamma_2+\sin^2\theta_0)}{i\pi(\gamma_1+\gamma_2)(\alpha - k\cos\theta_0)} \tag{15}$$

where

$$K_1(\alpha) = \left[\frac{k}{\Gamma(\alpha)}+\frac{1}{\gamma}\right]^{-1}$$

$$K_2(\alpha) = \left\{\left[\frac{k}{\Gamma(\alpha)}+\frac{1}{\gamma_1}\right]\cdot\left[\frac{k}{\Gamma(\alpha)}+\frac{1}{\gamma_2}\right]\right\}^{-1}. \tag{16}$$

By following the standard Wiener–Hopf procedure, the solution is obtained as [6]

$$\Phi_1^+(\alpha) = -\frac{k\sin\theta_0}{i\pi\gamma}\frac{K_1^+(\alpha)}{\Gamma^+(\alpha)}\frac{K_1^-(k\cos\theta_0)}{\Gamma^-(k\cos\theta_0)}\cdot\frac{1}{(\alpha - k\cos\theta_0)} \tag{17}$$

and

$$\Phi_2^+(\alpha) = -\frac{1}{i\pi}\frac{k(\gamma_1+\gamma_2)}{(\gamma_1\gamma_2)}\frac{K_2^+(\alpha)}{\Gamma^+(\alpha)}\frac{K_2^-(k\cos\theta_0)}{\Gamma^-(k\cos\theta_0)}\cdot\left[-\frac{k(\gamma_1\gamma_2+\sin^2\theta_0)}{(\gamma_1+\gamma_2)(\alpha - k\cos\theta_0)}+c\right]. \tag{18}$$

Here $K_{1,2}^+(\alpha)$ and $K_{1,2}^-(\alpha)$ denote the Wiener–Hopf factors of $K_{1,2}(\alpha)$ which are regular in the upper and lower α-planes, respectively. The explicit expressions in terms of Maliuzhinetz's function for the factorization of a similar function was first given by Senior [1]. By replacing $(1/\gamma)$ in $K_1(\alpha)$ with (η) it can easily be seen that the function $K(\zeta)$ given by Senior (see (6) in [1]) is identical to $K_1(\alpha)$. Also, it is obvious that $K_2(\alpha)$ is composed of the product of two functions of $K_1(\alpha)$ type. The main steps of the factorization of such a function in terms of Maliuzhinetz's function is outlined in [7]. The split factors of $\Gamma(\alpha)$ have the same analytical properties as $K_{1,2}^{\pm}(\alpha)$and their explicit expressions are $\Gamma^{\pm}(\alpha) = \sqrt{k \pm \alpha}$.

As is seen, edge conditions are not sufficient to determine the unknowns; the solution still involves an unknown constant after the application of the classical edge conditions. Although several approaches have been introduced by various authors [8], [9] for determining the unknowns which arise from the higher order derivatives involved by the approximate boundary conditions, Senior [10]–[12] has given a systematic method for determining the unknown constants using constraints imposed on the currents or the scattered fields. This method implies that the normal component of the electric current vanishes at the edge which leads to certain continuity requirements on the field components at the edge. This approach is also used in the present study, and the unknown constant is derived as

$$k(\gamma_1+\gamma_2)c = k\cos\theta_0 + s_0\frac{k(\gamma_1+\gamma_2)[K_2^+(s_0)]^2 - \gamma_1\gamma_2[\Gamma^+(s_0)]^2}{k(\gamma_1+\gamma_2)[K_2^+(s_0)]^2 + \gamma_1\gamma_2[\Gamma^+(s_0)]^2} \tag{19}$$

with $s_0^2 = k^2(1+\gamma_1\gamma_2)$ which completes the solution of the Wiener–Hopf problem given by (14) and (15).

III. Field Analysis

The scattering field analysis, based on the integrals in (9), requires to determine the spectral coefficients $M(\alpha)$ and $N(\alpha)$, which can easily be obtained from (12) and (13)

$$M(\alpha) = \tfrac{1}{2}[\Phi_1^+(\alpha) + \Phi_2^+(\alpha)/\Gamma(\alpha)]$$

and

$$N(\alpha) = -\tfrac{1}{2}[\Phi_1^+(\alpha) - \Phi_2^+(\alpha)/\Gamma(\alpha)]. \tag{20}$$

Now, by substituting $M(\alpha)$ and $N(\alpha)$ expressions into (9), the scattering field integrals can be found as

$$H_z^s(r,\theta) = \mp\frac{k}{2\pi i}\int_L\left\{\frac{K_1^+(\alpha)}{\Gamma^+(\alpha)}\frac{K_1^-(k\cos\theta_0)}{\Gamma^-(k\cos\theta_0)}\cdot\frac{\sin\theta_0}{\gamma(\alpha - k\cos\theta_0)} \pm \frac{K_2^+(\alpha)}{\Gamma^+(\alpha)\Gamma(\alpha)}\frac{K_2^-(k\cos\theta_0)}{\Gamma^-(k\cos\theta_0)}\cdot\frac{1}{\gamma_1\gamma_2}\left[-\frac{k(\gamma_1\gamma_2+\sin^2\theta_0)}{(\alpha - k\cos\theta_0)}+c(\gamma_1+\gamma_2)\right]\right\}\cdot e^{\pm i\Gamma(\alpha)y - i\alpha x}\,d\alpha \tag{21}$$

where the upper and the lower signs in (21) correspond to the integrals for regions $y > 0$ and $y < 0$, respectively. By applying the standard saddle-point method, the diffracted field

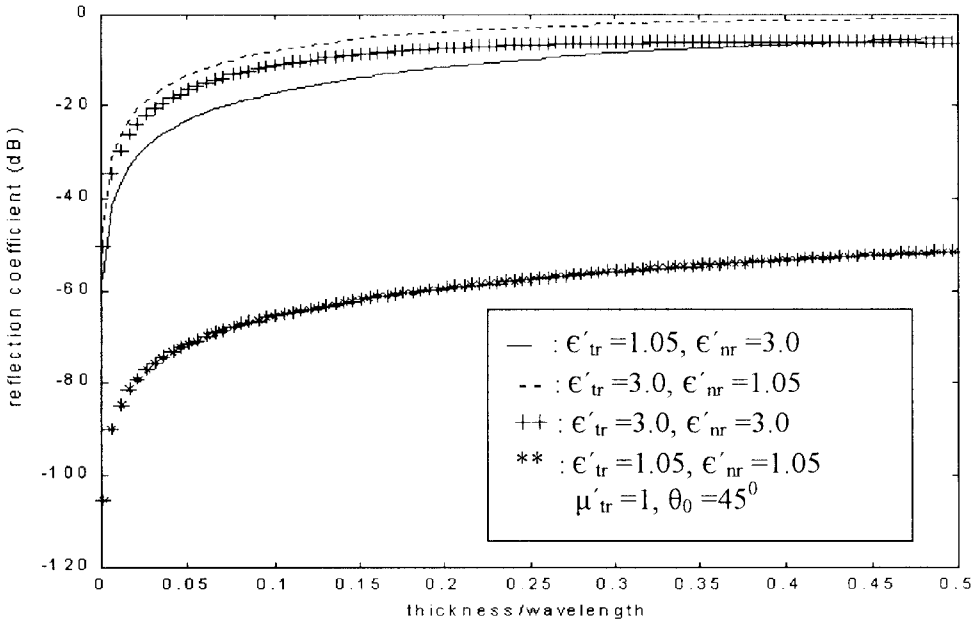

Fig. 4. Variation of reflection coefficient in decibels with $\mu'_{tr} = 1. \theta_0 = 45^\circ$ for H polarization.

expressions are obtained as

$$H_z^d(r, \theta, \theta_0) = D^d(\theta, \theta_0)\frac{e^{ikr}}{\sqrt{kr}} \tag{22}$$

with

$$D^d(\theta, \theta_0) = \frac{e^{i\pi/4}}{\sqrt{2\pi}}\left\{\frac{1}{\gamma_1\gamma_2}\frac{K_2^-(k\cos\theta_0)K_2^-(k\cos\theta)}{\sqrt{1-\cos\theta}\sqrt{1-\cos\theta_0}} \cdot\left[\frac{\gamma_1\gamma_2+\sin^2\theta_0}{(\cos\theta+\cos\theta_0)}+(\gamma_1+\gamma_2)c\right] \mp \frac{K_1^-(k\cos\theta_0)K_1^-(k\cos\theta)}{\sqrt{1-\cos\theta}\sqrt{1-\cos\theta_0}}\frac{AZ_0\sin\theta_0\sin\theta}{(\cos\theta+\cos\theta_0)}\right\}. \tag{23}$$

The pole contributions at $t = \pi \mp \theta_0$ give the reflected and transmitted fields which are present for $y > 0$ and $y < 0$ regions, respectively (see Fig. 2). The reflection and transmission coefficients are derived easily as

$$T^{(r)}(\theta_0) = \frac{AZ_0\sin\theta_0}{1+AZ_0\sin\theta_0} - \frac{C-ikDZ_0\cos^2\theta_0}{C-Z_0\sin\theta_0-ikDZ_0\cos^2\theta_0} \tag{24}$$

and

$$T^{(t)}(\theta_0) = \frac{1}{1+AZ_0\sin\theta_0} - \frac{C-ikDZ_0\cos^2\theta_0}{C-Z_0\sin\theta_0-ikDZ_0\cos^2\theta_0} \tag{25}$$

where the superscripts d, r, and t denote the terms corresponding to diffraction, reflection and transmission, respectively. This concludes the analysis of the field giving the total field as follows:

$$H_z(r, \theta) = \begin{cases} H_z^i(r, \theta) + H_z^r(r, \theta) + H_z^d(r, \theta) \\ \quad 0 < \theta < (\pi - \theta_0) \\ H_z^i(r, \theta) + H_z^d(r, \theta) \\ \quad (\pi - \theta_0) < \theta < (\pi + \theta_0) \\ H_z^d(r, \theta) + H_z^t(r, \theta) \\ \quad (\pi + \theta_0) < \theta < 2\pi. \end{cases} \tag{26}$$

Although the analysis is carried out for the H-polarized case, the field expressions can easily be obtained by duality for E polarization. By substituting $E \to H$, $H \to -E$, $\epsilon'_{tr} \leftrightarrow \mu'_{tr}$ and $\epsilon'_{nr} \leftrightarrow \mu'_{nr}$ due to the duality principle the following:

$$D^d(\theta, \theta_0) = \frac{e^{i\pi/4}}{\sqrt{2\pi}}\left\{\frac{1}{\gamma_1\gamma_2}\frac{K_2^-(k\cos\theta_0)K_2^-(k\cos\theta)}{\sqrt{1-\cos\theta}\sqrt{1-\cos\theta_0}} \cdot\left[\frac{\gamma_1\gamma_2+\sin^2\theta_0}{(\cos\theta+\cos\theta_0)}+(\gamma_1+\gamma_2)c\right] \pm \frac{C}{Z_0}\frac{K_1^-(k\cos\theta_0)K_1^-(k\cos\theta)}{\sqrt{1-\cos\theta}\sqrt{1-\cos\theta_0}} \cdot\frac{\sin\theta_0\sin\theta}{(\cos\theta+\cos\theta_0)}\right\} \tag{27}$$

is obtained for the diffraction coefficient where the upper and lower signs correspond to the $y > 0$ and $y < 0$ regions, respectively. The reflection and transmission coefficients are

$$T^{(r)}(\theta_0) = -\left[\frac{AZ_0+ikB\cos^2\theta_0}{AZ_0+\sin\theta_0+ikB\cos^2\theta_0} + \frac{C\sin\theta_0}{C\sin\theta_0-Z_0}\right] \tag{28}$$

and

$$T^{(t)}(\theta_0) = \frac{\sin\theta_0}{AZ_0+\sin\theta_0+ikB\cos^2\theta_0} + \frac{C\sin\theta_0}{Z_0-C\sin\theta_0} \tag{29}$$

where the total field is obtained as given by (26).

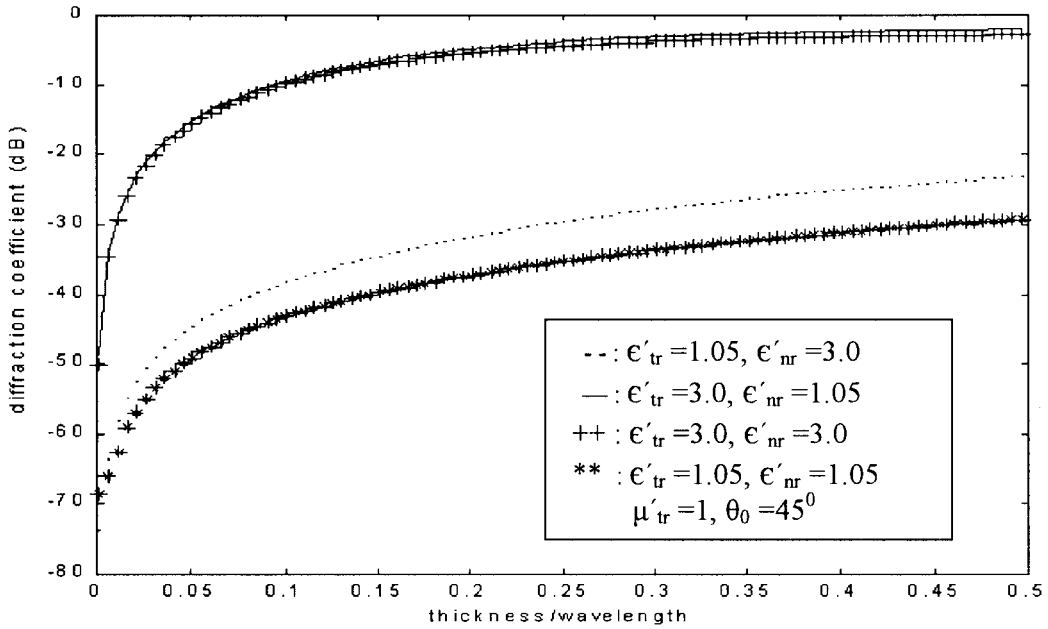

Fig. 5. Variation of diffraction coefficient in decibels with $\mu'_{tr} = 1$, θ_0° and $\theta = 100^\circ$ for H polarization.

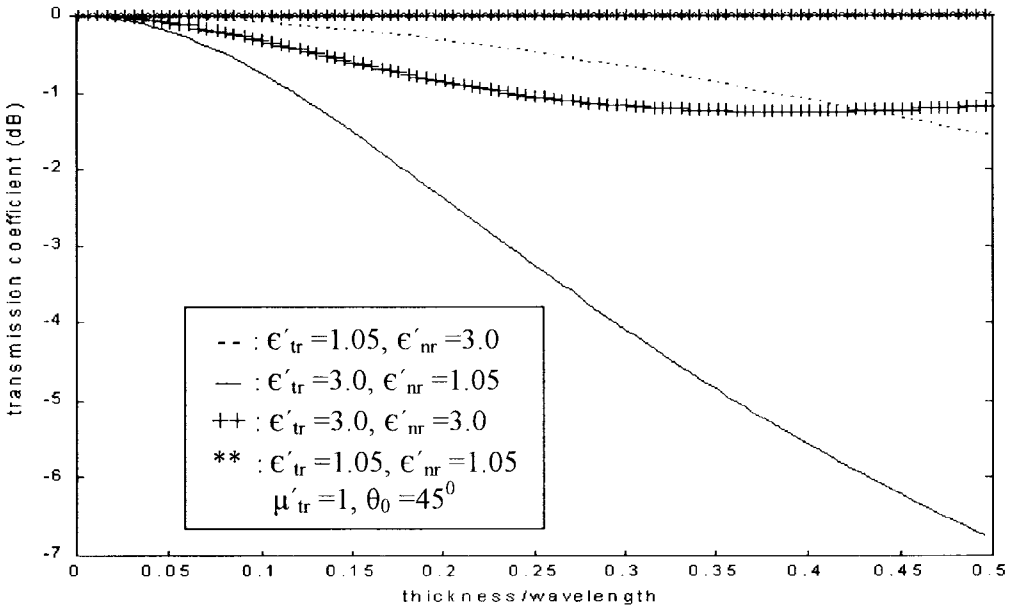

Fig. 6. Variation of transmission coefficient in decibels with μ'_{tr} and $\theta_0 = 45^\circ$.

IV. Numerical Results

By using the definitions of the constitutive parameters

$$A = -\frac{ikh}{Z_0}(\epsilon'_{tr} - 1)$$
$$C = ikhZ_0(\mu'_{tr} - 1)$$
$$D = -h\frac{\epsilon'_{nr} - 1}{\epsilon'_{nr}}$$
$$\gamma_1\gamma_2 = -\frac{\epsilon'_{nr}(\mu'_{tr} - 1) + (\epsilon'_{nr} - 1)}{\epsilon'_{nr} - 1}$$
$$\gamma_1 + \gamma_2 = -\frac{i\epsilon'_{nr}}{kh(\epsilon'_{nr} - 1)}$$
$$\gamma = 1/AZ_0 = \frac{i}{kh(\epsilon'_{tr} - 1)}$$

are obtained for the H polarized case. In the nonmagnetic case ($\mu'_{tr} = 1$), the following simplifications $C = 0$, $s_0 = 0$, $(\gamma_1 + \gamma_2)c = \cos\theta_0$, $\gamma_1\gamma_2 = -1$ can be made and from (23)–(25)

$$D^d(\theta, \theta_0) = -\frac{e^{i\pi/4}}{\sqrt{2\pi}}\left[\frac{K_2^-(k\cos\theta_0)K_2^-(k\cos\theta)}{\sqrt{1-\cos\theta_0}\sqrt{1-cos\theta}} \cdot \frac{\cos\theta\cos\theta_0}{(\cos\theta + \cos\theta_0)} \pm \frac{K_1^-(k\cos\theta_0)K_1^-(k\cos\theta)}{\sqrt{1-\cos\theta_0}\sqrt{1-cos\theta}} \cdot \frac{AZ_0\sin\theta_0\sin\theta}{(\cos\theta + \cos\theta_0)}\right] \quad (30)$$

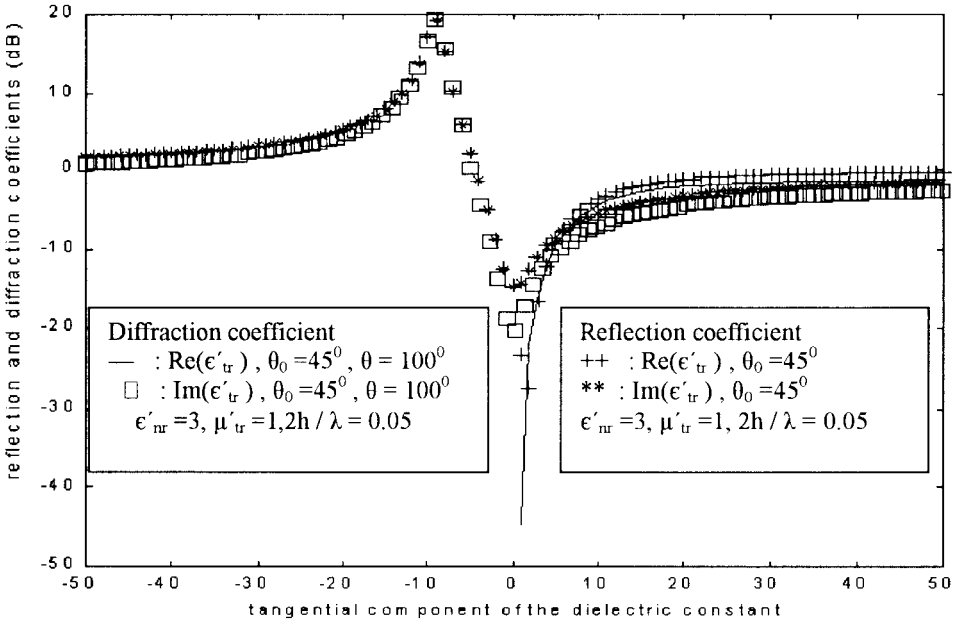

Fig. 7. Variation of reflection and diffraction coefficient in decibels with $\epsilon'_{nr} = 3$, $\mu'_{tr} = 1$, and $2h/\lambda = 0.05$ for H polarization.

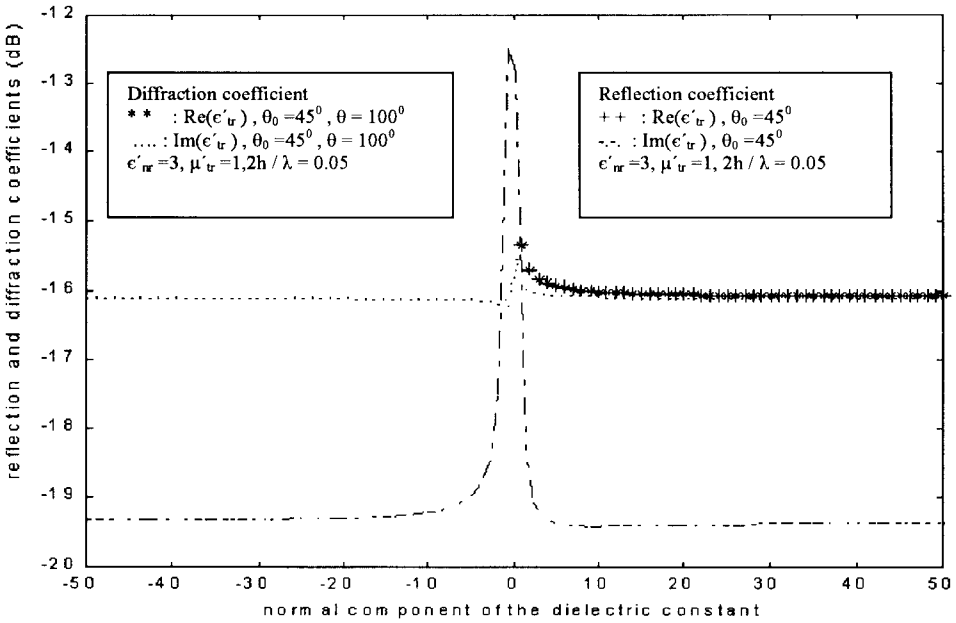

Fig. 8. Variation of reflection and diffraction coefficient in decibels with $\epsilon'_{nr} = 3$, $\mu'_{tr} = 1$, and $2h/\lambda = 0.05$ for H polarization.

for $y > 0$ and $y < 0$, respectively, and with

$$T^{(r)} = \frac{AZ_0 \sin\theta_0}{1 + AZ_0 \sin\theta_0} - \frac{ikD\cos^2\theta_0}{\sin\theta_0 + ikD\cos^2\theta_0} \tag{31}$$

and

$$T^{(t)} = \frac{1}{1 + AZ_0 \sin\theta_0} - \frac{ikD\cos^2\theta_0}{\sin\theta_0 + ikD\cos^2\theta_0}. \tag{32}$$

Some numerical examples for the nonmagnetic case under H polarization is obtained for reflection, transmission and diffraction coefficients given as $20\log_{10}|T^{(r)}|$, $20\log_{10}|T^{(t)}|$ and $20\log_{10}|D^{(d)}|$, respectively. The diffraction coefficients involve the split functions $K_1^{\pm}(\alpha)$ and $K_2^{\pm}(\alpha)$ which are written in terms of the Maliuzhinetz's function. By using the approximate formulas given by Volakis and Senior [13], Maliuzhinetz's function is expressed in a form convenient for numerical computation and, hence, the diffracted field coefficient is computed for different values of the constitutive parameters and for different thicknesses of the anisotropic layer.

First investigation is accomplished with respect to the thickness of the anisotropic dielectric layer in order to reveal the effectiveness of the simulation. From Figs. 4 and 5 it can be deduced that the optimum values of $2h/\lambda$ should be chosen between 0.05 and 0.15 to simulate the layer effectively with anisotropic dielectric layer boundary conditions. Also, it is seen that reflection and diffraction mechanisms are enhanced

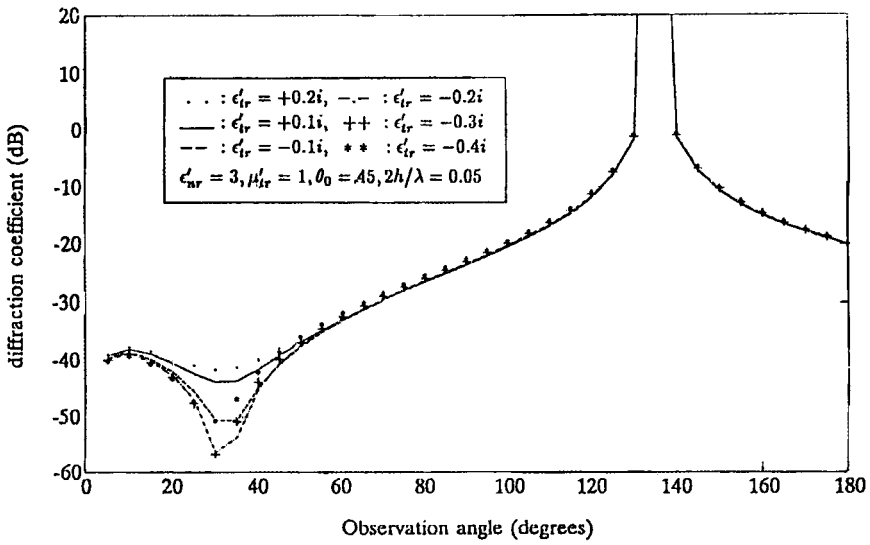

Fig. 9. Variation of diffraction coefficient in decibels with pure imaginary $\epsilon'_{tr} = 3$, $\mu'_{tr} = 1$, $= 1$, $\theta_0 = 45°$, and $2h/\lambda = 0.05$ for H polarization.

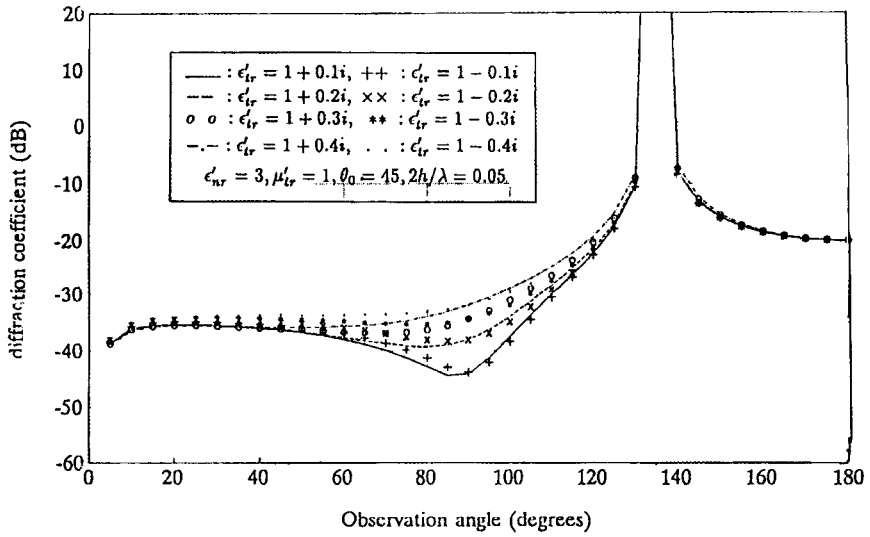

Fig. 10. Variation of diffraction coefficient in decibels with complex ϵ'_{tr} for $\epsilon_{nr} = 3$, $\mu'_{tr} = 1$, $\theta_0 = 45°$ and $2h/\lambda$.

for $\mathrm{Re}(\epsilon'_{tr}) > \mathrm{Re}(\epsilon'_{nr})$ cases, which means that the effect of $\mathrm{Re}(\epsilon'_{tr})$ is dominant. Fig. 6 shows the variation of the transmission coefficient, and its comparison with Figs. 4 and 5 verifies the interpretation of reflection and diffraction with respect to ϵ'_{tr} and ϵ'_{nr}; so, transmission is stronger for smaller $\mathrm{Re}(\epsilon'_{tr})$ values. On the other hand, almost all of the incident wave is transmitted through the layer for $\epsilon'_{tr} = \epsilon'_{nr} = 1.05$, while the reflected and diffracted field components take very small values, as expected.

A second investigation is done with respect to the physical parameters of the anisotropic dielectric layer. As is seen from $T^{(r)}$ and $T^{(t)}$ expressions given by (31) and (32), respectively, $(1 + AZ_0 \sin\theta_0)$ may become maximum for certain value of ϵ'_{tr} while $[\sin\theta_0 + ikD\cos^2\theta_0]$ may yield a maximum value for ϵ'_{nr}, which correspond to resonances in the layer. Fig. 7 denotes the variation of reflection and diffraction coefficients for $\epsilon'_{nr} = 3$, $\mu'_{tr} = 1$ and $2h/\lambda = 0.05$. For these parameter values with $\theta_0 = 45^o$, $(1 + AZ_0 \sin\theta_0) = 0$ yield $\epsilon'_{tr} = 1 - 9i$, and as expected, $\mathrm{Im}(\epsilon'_{tr}) = -9$ corresponds to a resonance value both for reflection and diffraction. Also, reflected and diffracted fields are strengthened as ϵ'_{tr} is increased for $\mathrm{Re}(\epsilon'_{tr}) > 1$ and $\mathrm{Im}(\epsilon'_{tr}) > 0$. On the other hand, Fig. 8 shows that diffraction and reflection are decreased as (ϵ'_{nr}) is increased for $\mathrm{Re}(\epsilon'_{nr}) > 1$ and $|\mathrm{Im}(\epsilon'_{nr})| > 0$. Note that the curve corresponding to the variation of the diffraction coefficient with respect to $\mathrm{Re}(\epsilon'_{nr})$ coincides with the reflection coefficient curve.

A third group of investigation consists of variation of diffraction coefficient with respect to the observation angle for various values of physical parameters. From Fig. 7 it is obvious that minimum reflection and diffraction effects correspond to the case when $\mathrm{Re}(\epsilon'_{tr}) \approx 1$. Since, for engineering applications, it is of interest to minimize these effects, the variation of diffraction coefficient with respect to observation angle for very small negative and positive values of $\mathrm{Im}(\epsilon'_{tr})$ is investigated. Due to the symmetry, only

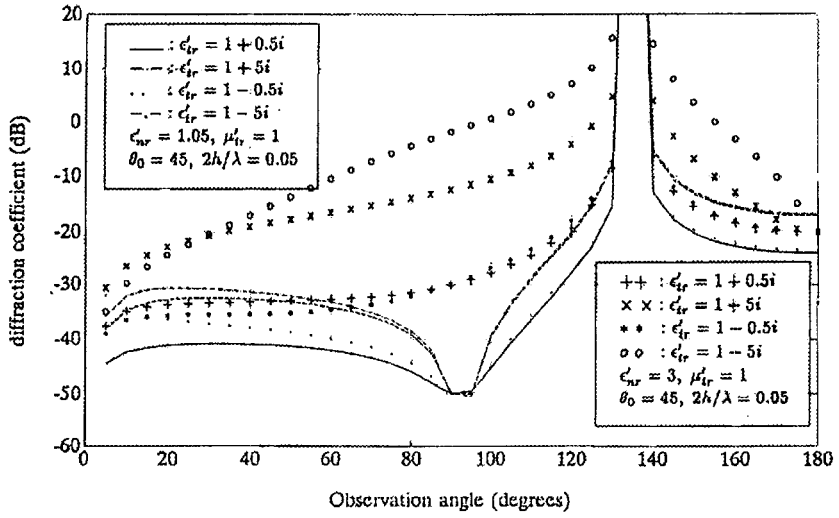

Fig. 11. Variation of diffraction coefficient in decibels with $\mu'_{tr} = 1$, $\theta_0 = 45^o$ $2h/\lambda = 0.05$ in H polarization case for $\epsilon'_{nr} = 1.05$ and $\epsilon'_{nr} = 3$.

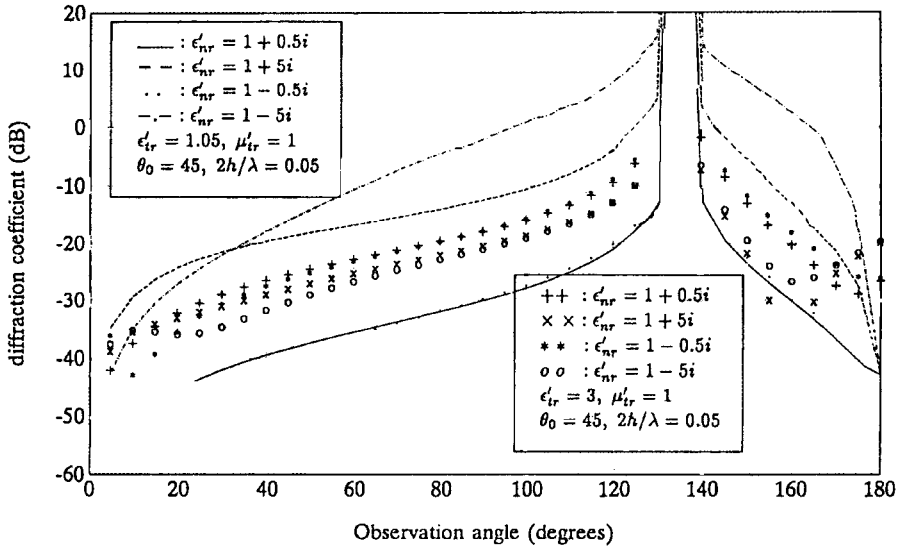

Fig. 12 Variation of diffraction coefficient in decibels with $\mu'_{tr} = 1$, $\theta_0 = 45^\circ$, $2h/\lambda = 0.05$ in H polarization case for $\epsilon'_{nr} = 1.05$ and $\epsilon'_{nr} = 3$.

variation for $\theta \in (0^\circ, 180^\circ)$ is shown in Figs. 9–12. As is expected, diffraction effects are suppressed at all observation angles while for a small angular section around $\theta = 30^\circ$ the attenuation is much higher corresponding to a considerable amount of energy absorption (see Fig. 9). Another interesting observation is that diffraction coefficient becomes minimum for a certain value of $\mathrm{Im}(\epsilon'_{tr})$ in this angular section. The location of the region of depression depends on the constitutive parameters of the dielectric layer. This behavior is displayed in Fig. 10 by inserting a small real part to ϵ'_{tr} and varying $\mathrm{Im}(\epsilon'_{tr})$ in the range where the diffraction coefficient passes through a minimum. On the other hand, the interdependence of ϵ'_{tr} and ϵ'_{nr} on effecting the diffraction mechanism is explicitly seen from Figs. 11 and 12. Although the depression region is present for larger values of $|\mathrm{Im}(\epsilon'_{tr})|$ when $\epsilon'_{nr} = 1.05$, it disappears when ϵ'_{nr} is increased (see Fig. 11). The comparison of the graphs in Fig. 11 shows that diffraction is gradually decreased as ϵ'_{nr} is increased while it is strengthened for negative values of $\mathrm{Im}(\epsilon'_{tr})$ due to the resonance effect. It is seen from Fig. 12 that the magnitude of ϵ'_{nr} is dominantly effective when $\epsilon'_{tr} = 1.05$. But an interesting influence is observed with an increase in ϵ'_{tr}, and the stronger field values of the previous case are depressed, while the weaker ones are enhanced for $\epsilon'_{tr} = 3$.

The diffraction coefficients given in (23) and (27) are not uniform and it is expected that the field will take very large values in the transition regions which are determined by the incidence angle as $(\pi - \theta_0)$ and $(\pi + \theta_0)$.

For the nonmagnetic isotropic case ($\mu'_{tr} = 1$, $\epsilon'_{tr} = \epsilon'_{nr}$), the reflection and transmission coefficients given in (31) and (32) are reduced to the following:

$$T^{(r)} = \frac{AZ_0 \sin\theta_0}{1 + AZ_0 \sin\theta_0} - \frac{AZ_0 \cos^2\theta_0}{\epsilon'_{tr} \sin\theta_0 + AZ_0 \cos^2\theta_0} \quad (33)$$

and

$$T^{(t)} = \frac{1}{1 + AZ_0 \sin\theta_0} - \frac{AZ_0 \cos^2\theta_0}{\epsilon'_{tr} \sin\theta_0 + AZ_0 \cos^2\theta_0} \quad (34)$$

where the reflection coefficient is identical to (29) in [3]. It can easily be shown that the boundary conditions given by (1) and (2) for simulating an anisotropic dielectric layer can be reduced to the modified resistive sheet and conductive sheet conditions for the isotropic case [3].

V. Conclusions

In this paper, the problem of an anisotropic thin dielectric layer illuminated by an H-polarized plane wave has been solved and a nonuniform expression for the edge diffraction coefficient has been derived. The solution was accomplished by using a pair of boundary conditions to model an anisotropic thin dielectric layer as an infinitesimally thin sheet. This leads to a pair of uncoupled Wiener–Hopf equations whose solution can be expressed in terms of Maliuzhinetz's function. The uniqueness of the solution is achieved by using an edge constraint in addition to the classical edge conditions. The results are compared with the previously obtained ones for $\epsilon'_{tr} = \epsilon'_{nr}$ and $\mu'_{tr} = \mu'_{nr}$ and it has been shown that they are in good agreement. As a consequence, the electric and magnetic characteristics of the anisotropic dielectric layer in normal and parallel directions can be considered to be different from each other, this can give a lot of freedom to the designer. For example, it can be possible to consider the dielectric constants of the layer in parallel and perpendicular directions as different or vice versa. It has been determined numerically that the simulation by anisotropic dielectric layer boundary conditions is effective for $0.05 \leq 2h/\lambda \leq 0.15$. Also, it has been shown that the effect of ϵ'_{tr} on scattering mechanism is dominant compared to that of ϵ'_{nr}.

Acknowledgment

The authors would like to thank A. Büyükaksoy and J. Burkholder together with the anonymous referees for their helpful comments and suggestions. They would also like to thank A. Vahap Saygin for reproduction of the curves presented in this paper.

References

[1] T. B. A. Senior, "Half-plane edge diffraction," *Radio Science,* vol. 10, pp. 645–650, 1975.
[2] I. Anderson, "Wave diffraction by a thin dielectric half-plane," *IEEE Trans. Antennas Propagat.,* vol. AP-27, pp. 584–589, May 1979.
[3] T. B. A. Senior and J. L. Volakis, "Sheet simulation of a thin dielectric layer," *Radio Sci.,* vol. 22, pp. 1261–1272, 1987.
[4] M. İdemen, " Straightforward derivation of boundary conditions on sheet simulating an anisotropic thin layer," *Electron. Lett.,* vol. 24, pp. 663–665, 1988.
[5] T. B. A. Senior and J. L. Volakis, *Approximate Boundary Conditions in Electromagnetics.* London, U.K.: Inst. Elect. Eng., 1995.
[6] A. H. Serbest and A. Yazici, " Plane wave diffraction by an anisotropic dielectric half plane," in *IEEE AP-S Int. Symp.,* Ontario, Canada, June 1991, pp. 562–565.
[7] M. G. Uzgören, A. Büyükaksoy, and A. H. Serbest, "Diffraction coefficient related to a discontinuity formed by impedance and resistive half-planes," *Proc. Inst. Elect. Eng.,* vol. 136, pt. H, no. 1, pp. 19–23, 1989.
[8] F. G. Leppington, "Travelling waves in a dielectric slab with an abrupt change in thickness," *Proc. Roy. Soc. London,* vol. A386, pp. 443–460, 1983.
[9] R. G. Rojas and Z. Al-hekail, "Generalized impedance/resistive boundary conditions for electromagnetic scattering problems," *Radio Sci.,* vol. 24, pp. 1–12, 1989.
[10] T. B. A. Senior, "Generalized boundary and transition conditions and the question of uniqueness," *Radio Sci.,* vol. 27, pp. 929–934, 1992.
[11] ——, "Generalized boundary and transition conditions and uniqueness of solution," Univ. Michigan, Ann Arbor, Radiation Lab. Rep. RL 891, 1993.
[12] ——,"Diffraction by half plane junction," Univ. Michigan, Ann Arbor, Radiation Lab. Rep. RL 892, 1993.
[13] J. L. Volakis and T. B. A. Senior, "Simple expressions for a function occurring in diffraction theory," *IEEE Trans. Antennas Propagat.,* vol. AP-33, pp. 678–680, 1985.

Arslan Yazici (M'94) deceased, was born in Yozgat, Turkey, on November 1, 1950. He received the B.S. degree in electronics engineering from the Technical University of Istanbul, Turkey, in 1975, and the M.S. and Ph.D. degrees in electronics engineering from Cukurova University, Adana, Turkey, in 1990 and 1994, respectively.

He joined the Department of Electrical and Electronics Engineering, Cukurova University, Adana, Turkey, in 1988. From 1975 to 1988 he was employed by PTT (Post, Telephone, and Telegraph) Office of Turkey, Adana, as an Engineer and Director at different levels. At Cukurova University, he served as Lecturer from 1988 to 1994 and as Assistant Professor after 1994 during which time he made very important contributions to the activities to the Department of Education and Research. His special interest was in the Wiener–Hopf technique and its applications to high-frequency diffraction problems.

Dr. Yazici was a member of the Turkish Chamber of Electrical Engineers.

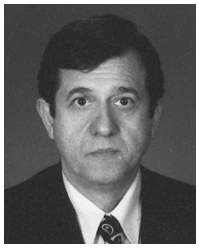

A. Hamit Serbest (M'83–SM'92) was born in Adana, Turkey, on March 24, 1953. He received the B.S., M.S., and Ph.D. degrees in electronics engineering from Technical University of Istanbul, Turkey, in 1975, 1977, and 1982, respectively.

From 1975 to 1981, he worked as a Research Assistant at Faculty of Electrical Engineering, Technical University of Istanbul and later joined Cukurova University where he became Associate Professor in 1985 and a Full Professor in 1991. He was founder of Department of Electrical and Electronics Engineering, Cukurova University, in 1987 and has served as Department Head since then. Currently, he has served as Dean of Faculty of Engineering and Architecture since 1995. He worked as Visiting Scientist from 1991 to 1992 at Institute of Radio Frequency Technology of German Aerospace Research Establishment (DLR) through an Alexander von Humboldt Foundation Fellowship. From 1993 to 1995, he was employed as Project Coodinator in Microwave Remote Sensing Division of Department of Space Sciences in Marmara Research Center of TUBITAK (Scientific and Technical Research Council of Turkey). His areas of research interest are mixed boundary value problems in diffraction theory, Wiener–Hopf technique and high-frequency diffraction techniques.

Dr. Serbest is Chairman of Commission-B of Turkish Committee of URSI, and a member of Electromagnetics Academy.